

---

# MULTI-OBJECTIVE MODEL-BASED REINFORCEMENT LEARNING FOR INFECTIOUS DISEASE CONTROL

---

Runzhe Wan Xinyu Zhang Rui Song  
Department of Statistics  
North Carolina State University  
{rwan, xzhang97, rsong}@ncsu.edu

## ABSTRACT

Severe infectious diseases such as the novel coronavirus (COVID-19) pose a huge threat to public health. Stringent control measures, such as school closures and stay-at-home orders, while having significant effects, also bring huge economic losses. In the face of an emerging infectious disease, a crucial question for policymakers is how to make the trade-off and implement the appropriate interventions timely given the huge uncertainty. In this work, we propose a Multi-Objective Model-based Reinforcement Learning framework to facilitate data-driven decision-making and minimize the overall long-term cost. Specifically, at each decision point, a Bayesian epidemiological model is first learned as the environment model, and then the proposed model-based multi-objective planning algorithm is applied to find a set of Pareto-optimal policies. This framework, combined with the prediction bands for each policy, provides a real-time decision support tool for policymakers. The application is demonstrated with the spread of COVID-19 in China.

## 1 Introduction

The novel coronavirus (COVID-19) has spread rapidly and posed a tremendous threat to the global public health (Organization et al., 2020). Among the efforts to contain its spread, several strict control measures, including school closures and workplace shutdowns, have shown high effectiveness (Anderson et al., 2020). Nevertheless, these measures bring enormous costs to economies and other public welfare aspects at the same time (Eichenbaum et al., 2020). For example, an unprecedented unemployment rate in the United States partially caused by some COVID-19 control measures is anticipated by economists (Gangopadhyaya and Garrett, 2020). In the face of an emerging infectious disease, there are usually multiple objectives conflicting with each other, and either overreaction or under-reaction may result in a substantial unnecessary loss. A crucial question for policymakers all around the world is *how to make the trade-off and intervene at the right time and in the right amount to minimize the overall long-term cost to the citizens.*

This work is motivated by the ongoing COVID-19 pandemic, where it is witnessed that the decision-making can be impeded by huge intervention costs, great uncertainty on the infectious ability of the disease and the effectiveness of different interventions, and various concerns over the long-term impacts. This paper aims to provide a real-time data-driven decision support framework for policymakers. We formalize the problem under the multi-objective Markov decision process (MOMDP) framework and integrate epidemiology models, statistical methods, and reinforcement learning algorithms to address this problem.

**Contribution.** Our contributions are multi-fold. First, as our transition model, we generalize the celebrated Susceptible-Infected-Removal (SIR) model (Kermack and McKendrick, 1927) to allow simultaneous estimation of the infectious ability of this disease and evaluation for the effectiveness of different control measures, in an online fashion. There is a vast literature on modeling and prediction for infectious diseases; see (Keeling and Rohani, 2011) for an overview. Among these works, compartmental models such as the SIR model are widely used; see, e.g., (Song et al., 2020a) and (Sun et al., 2020) for applications to COVID-19. During an outbreak, the knowledge about the infectious ability and the effectiveness of interventions usually change a lot, and a quantitative decision-making support tool should utilize the

---

This paper is accepted at the 27th ACM SIGKDD Conference on Knowledge Discovery and Data Mining (KDD 2021). The authors are grateful to the anonymous reviewers for valuable comments and suggestions.

update-to-date information timely. However, none of these works considers online parameter updating and intervention effect estimation at the same time. We aim to achieve this goal via an online Bayesian framework.

Second, we propose a novel online planning framework to assist policymakers in making decisions that minimize the overall long-term cost. In real applications, policymakers generally group different interventions into several ordered levels with increasing strictness and choose among them subsequently (e.g., in the U.S. (Korevaar et al., 2020) and New Zealand (Wilson, 2020)). This paper will focus on selecting among such a set of ordinal actions. Specifically, at each decision point, on the ground of the estimated generalized SIR model, we propose a model-based planning algorithm to learn the optimal intervention policy, for each given weight between the two competing objectives, i.e., minimizing the epidemiological cost and the economic cost. Both interpretable policy classes and complex black-box classes are considered. We then extend the algorithm to obtain a representative set of Pareto-optimal policies, i.e., policies that cannot be improved for one objective without sacrificing another. This framework, combined with the prediction bands for each policy, achieves the goal of supporting multi-objective decision-making. Compared with the huge literature on infectious disease modeling and prediction, the optimal decision-making problem is far less studied. Most works either focus on the evaluation of several fixed interventions (Tildesley et al., 2006; Ferguson et al., 2020; Hellewell et al., 2020) or study the optimal control problem with a deterministic model (Ledzewicz and Schättler, 2011; Elhia et al., 2013). None of these works allows sequential decision making with online updated parameter estimation, which enables selecting the appropriate intervention according to the current state and available data. In addition, the long-term effect is particularly important in this application due to the spread nature of the pandemic. Reinforcement learning (RL) is particularly suitable for these purposes, while its application in infectious disease control is relatively new to the literature. The existing works are mainly concerned with problems caused by limited resources (Probert et al., 2018; Laber et al., 2018), such as vaccine limitations in controlling seasonal flu. In contrast, we focus on another aspect, the multi-objective problem caused by the huge costs of stringent control measures. This approach provides us with a clearer view of the trade-off. To our knowledge, this is the first work on applications of multi-objective RL to infectious disease control.

Third, we present an application of our method to control the outbreak of COVID-19 as an example, which is important in its own right. Our proposed framework is generally applicable to pandemic controls. To investigate the robustness, applications to other diseases and several sensitivity analyses are also studied.

**Related work.** In addition to the aforementioned literature on infectious disease-related modeling, our methodology also belongs to the field of reinforcement learning. Our problem is closely related to the line of research on MOMDPs (see (Roijers et al., 2013) or (Liu et al., 2014) for a survey), which studies problems with multiple competing objectives. When the weights between objectives are unknown, the literature focuses on obtaining the whole class of Pareto-optimal policies approximately (Castelletti et al., 2012; Barrett and Narayanan, 2008; Parisi et al., 2017; Pirotta et al., 2015). Because of the online planning nature in our case, it suffices to adopt a simpler approach, by performing multiple runs of policy search over a representative set of weights (Van Moffaert et al., 2013; Natarajan and Tadepalli, 2005).

Besides, RL algorithms are commonly classified as model-based methods (e.g., MBVE (Feinberg et al., 2018), MCTS (Browne et al., 2012), etc.), which directly learn a model of the system dynamics, and model-free methods (e.g., fitted-Q iteration (Riedmiller, 2005), deep-Q network (Mnih et al., 2015), actor-critic (Konda and Tsitsiklis, 2000), etc.), which do not. In the case of emerging infectious disease control, on one hand, the algorithm needs to generalize to unseen transitions (e.g., the end of the epidemic), where the model-free approach is typically not applicable (van Hasselt et al., 2019); on the other hand, some epidemiological models have demonstrated satisfactory prediction power. Therefore, the model-based approach is adopted in this paper.

Finally, we note that some efforts have been made in the literature to study the control policy for COVID-19 (Alvarez et al., 2020; Piguillem and Shi, 2020; Eftekhari et al., 2020). As discussed above, these works did not consider the multi-objective problem. In addition, they focus on solving a one-time planning problem to decide all future actions instead of providing a real-time decision-making framework. RL algorithms have also been applied to learn the vaccine distribution strategy (Awasthi et al., 2020) or to control mobility (Song et al., 2020b).

**Outline.** The remainder of this paper is structured as follows. We first introduce some background of sequential decision-making and epidemiological modeling in Section 2. The proposed decision-making workflow is outlined in Section 3, with details of several components discussed in Section 4. The numerical experiments are presented in Section 5. We conclude the paper with discussions and possible extensions in Section 6.

## 2 Preliminary

### 2.1 Multi-objective Markov decision process

A Markov decision process (MDP) (Puterman, 2014) is a sequential decision making model which can be represented by a tuple  $\langle \mathcal{S}, \mathcal{A}, c, f \rangle$ , where  $\mathcal{S}$  is the state space,  $\mathcal{A}$  is the action space,  $c : \mathcal{S} \times \mathcal{A} \rightarrow \mathbb{R}$  is the expected cost function, and  $f : \mathcal{S}^2 \times \mathcal{A} \rightarrow \mathbb{R}$  is a Markov transition kernel. Throughout the paper we use the term *cost* instead of *reward*. A multi-objective MDP (MOMDP) is an extension of the MDP model when there are several competing objectives. An MOMDP can be represented as a tuple  $\langle \mathcal{S}, \mathcal{A}, \mathbf{c}, f \rangle$ , where the other components are defined as above and  $\mathbf{c} = (c^1, \dots, c^K)^T$  is a vector of  $K$  cost functions for  $K$  different objectives, respectively.

In this paper, we consider the finite horizon setting with a pre-specified horizon  $T$ . The horizon can simply be selected as a large enough number without loss of generality, since the costs we consider will be close to zero after the disease being controlled. Besides, we focus on deterministic policies for realistic consideration, since to assign an intervention by randomization may not be feasible. For a deterministic policy  $\pi$ , we define its  $k$ -th value function at time  $t_0$  as  $V_{k,t_0}^\pi(s) = \mathbb{E}_\pi(\sum_{t=t_0}^T c^k(S_t, A_t) | S_{t_0} = s)$ , where  $\mathbb{E}_\pi$  denotes the expectation assuming  $A_t = \pi(S_t)$  for every  $t \geq t_0$ .

In the MDP setting, the objective is typically to find an optimal policy  $\pi^*$  that minimizes the expected cumulative cost among a policy class  $\mathcal{F}$ . However, in an MOMDP, there may not be a single policy that minimizes all costs. Instead, we consider the set of Pareto-optimal policies with linear preference functions  $\Pi_{t_0} = \{\pi \in \mathcal{F} : \exists \omega \in \Omega \text{ s.t. } \omega^T \mathbf{V}_{t_0}^\pi(s) \leq \omega^T \mathbf{V}_{t_0}^{\pi'}(s), \forall \pi' \in \mathcal{F}, s \in \mathcal{S}\}$ , where  $\Omega = \{\omega \in \mathbb{R}_+^K : \omega^T \mathbf{1} = 1\}$  and  $\mathbf{V}_{t_0}^\pi = (V_{1,t_0}^\pi, \dots, V_{K,t_0}^\pi)^T$ . A policy is called *Pareto-optimal* if it can not be improved for one objective without sacrificing the others. The dependency on  $t_0$  is to be consistent with the online planning setting considered in this paper.

### 2.2 The Susceptible-Infected-Removal model

The compartmental models are, arguably, the most popular choices in epidemiology modeling (Tang et al., 2020). These models will divide the population into different compartments with labels, and model the transitions of people between these compartments to describe the mechanism of infectious diseases spread.

Among these models, the Susceptible-Infected-Removal (SIR) model is one of the most widely applied models (Brauer, 2008). Suppose at time  $t$ , the infectious disease is spread within  $N_t$  regions. Denote the total population of the  $l$ -th region as  $M_l$ , for  $l = 1, \dots, N_t$ . With the SIR model, we divide the total population into three groups: the individuals who can infect others, who have been removed from the infection system, and who have not been infected and are still susceptible. Denote the count for each group in region  $l$  at time  $t$  as  $X_{l,t}^S$ ,  $X_{l,t}^I$ , and  $X_{l,t}^R = M_l - X_{l,t}^S - X_{l,t}^I$ , respectively. We will discuss how to construct these variables using surveillance data in Section 4.1. The standard deterministic SIR model can then be written as a system of difference equations:

$$\begin{aligned} X_{l,t+1}^S &= X_{l,t}^S - \beta X_{l,t}^S X_{l,t}^I / M_l; \\ X_{l,t+1}^I &= X_{l,t}^I + \beta X_{l,t}^S X_{l,t}^I / M_l - \gamma X_{l,t}^I; \\ X_{l,t+1}^R &= X_{l,t}^R + \gamma X_{l,t}^I, \end{aligned}$$

where  $\beta$  and  $\gamma$  are constants representing the infection and removal rate, respectively. A diagram for the SIR model is given in Figure 1.

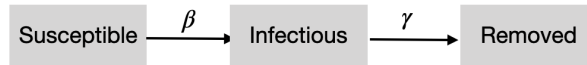
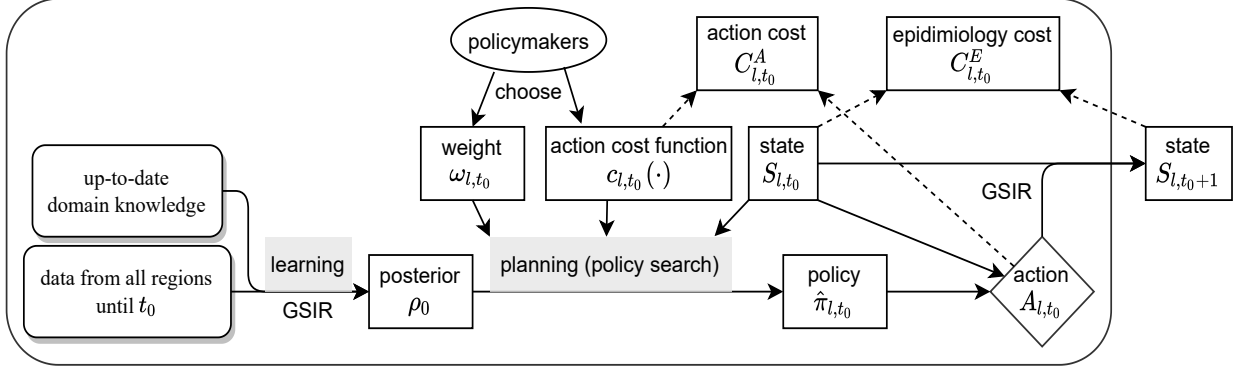


Figure 1: The infectious disease spread mechanism described by the SIR model.

## 3 Framework of the Decision Support Tool

In this section, we introduce the main framework. The transition model is first introduced in Section 3.1, and then the sequential decision-making problem for a given weight is defined in Section 3.2, with the multi-objective problem addressed in Section 3.3.


 Figure 2: Decision-making process for region  $l$  at time  $t_0$ 

### 3.1 The generalized SIR model

In this work, we aim to modify the SIR model as our transition model. We note that some other compartmental models such as the SEIR model (Brauer, 2008) can also fit in our framework. However, with limited data and knowledge in the face of an emerging infectious disease, the SIR model has been found to be a robust choice (Roda et al., 2020).

There are two limitations with the standard SIR model. First, the infection rate heavily depends on the control measure being taken. As discussed in Section 1, in this paper we focus on an ordinal set of actions  $\mathcal{A} = \{1, 2, \dots, J\}$ , with level 1 standing for no official measures. Second, a stochastic model with proper distribution assumptions is required to fit real data with randomness. Motivated by the discussions above, we propose the generalized SIR (GSIR) model and use it as our **transition model**:

$$\begin{aligned}
 X_{l,t+1}^S &= X_{l,t}^S - e_{l,t}^S, \quad e_{l,t}^S \sim \text{Poisson}\left(\sum_{j=1}^J \beta_j \mathbb{I}(A_{l,t} = j) X_{l,t}^S \frac{X_{l,t}^I}{M_l}\right); \\
 X_{l,t+1}^R &= X_{l,t}^R + e_{l,t}^R, \quad e_{l,t}^R \sim \text{Binomial}(X_{l,t}^I, \gamma); \\
 X_{l,t+1}^I &= M_l - X_{l,t+1}^S - X_{l,t+1}^R,
 \end{aligned} \tag{1}$$

where  $\mathbb{I}(\cdot)$  is the indicator function,  $A_{l,t}$  is the action taken by region  $l$  at time  $t$ , and  $\beta_j$  denotes the infection rate under action  $j$ . The choice of the Poisson and the Binomial distribution is popular in the literature (Held et al., 2019), and is motivated by their probabilistic implications. We assume  $\beta_1 \geq \beta_2 \geq \dots \geq \beta_J \geq 0$  to represent the increasing effectiveness. The estimation of  $\theta = (\gamma, \beta_1, \dots, \beta_J)^T$  is deferred to Section 4.2.

### 3.2 Sequential decision making

In this work, we focus on the intervention decision of each region: in the model estimation (learning) step, data from several similar regions are aggregated to share information and mitigate the issue that data is typically noisy, scarce, and single-episode in a pandemic; while in the decision-making (planning) step, each region chooses its own action.

**MOMDP definition.** The intervention decision-making problem can be naturally formalized as an MOMDP. For each region  $l$ , at each decision point  $t$ , according to the estimated transition model, the current **state**  $S_{l,t} = (X_{l,t}^S, X_{l,t}^I, X_{l,t}^R)^T$ , and their judgment, the policymakers determine a **policy**  $\pi_{l,t}$  with the objective of minimizing the overall long-term cost, and choose the **action**  $A_{l,t}$  to implement according to the policy. This action, assuming being effectively executed, will affect the infection rate during  $(t, t+1]$  and hence the conditional distribution of  $S_{l,t+1}$ . Let  $f(\cdot, \cdot; \theta)$  be the conditional density for  $S_{l,t+1}$  given  $S_{l,t}$  and  $A_{l,t}$  in model (1). In this work, we consider two cost variables, the **epidemiological cost**  $C_{l,t}^E$  and the **action cost**  $C_{l,t}^A$ .  $C_{l,t}^E$  can be naturally chosen as the number of new infections  $X_{l,t}^S - X_{l,t+1}^S$ . Let  $C_{l,t}^A = c_l(Z_{l,t}, A_{l,t}, Z_{l,t+1}) \in \mathbb{R}^+$  for a time-varying variable  $Z_{l,t}$  and a stochastic function  $c_l$ . Both  $c_l$  and  $Z_{l,t}$  should be chosen by domain experts. For example, with  $Z_{l,t}$  representing the unemployment rate,  $C_{l,t}^A = Z_{l,t+1} - Z_{l,t}$  can represent its change due to  $A_{l,t}$ . Since the modeling for action cost and its transition is a separate question, for simplicity, we focus on the case that  $C_{l,t}^A = c_l(A_{l,t})$  for a pre-specified stochastic function  $c_l(\cdot)$  in this paper.  $c_l(\cdot)$  is set to be region-specific to incorporate local features, such as the economic conditions. With a

given weight  $\omega_{l,t} \in \mathbb{R}^+$ , the **overall cost**  $C_{l,t}$  is then defined as  $C_{l,t}^E + \omega_{l,t}C_{l,t}^A$ . The expected cost functions can then be derived from these definitions, and for decision-making purposes, the overall cost is equivalent with the weighted cost defined in Section 2.1 when  $K = 2$ .

**Online planning.** The RL problem considered in this paper is an *online planning*, or sometimes called *planning at decision time* problem (Sutton and Barto, 2018), which focuses on selecting an action for the current state with collected environment information. We consider a sequence of decision points  $\mathcal{T} \subset \{1, \dots, T\}$  to reduce the action switch cost in real applications. At time  $t_0 \notin \mathcal{T}$ , the region keeps the same action with time  $t_0 - 1$ . At time  $t_0 \in \mathcal{T}$ , the policymakers choose an action according to the decision-making workflow displayed in Figure 2.

We summarize Figure 2 as follows. For each region  $l$ , at the decision point  $t_0$ , we first estimate the posterior of  $\theta$  as  $\rho_{t_0}$ , using accumulated data  $\mathcal{D}_{t_0} = \{S_{l,t}, A_{l,t}\}_{1 \leq l \leq N_{t_0}, 1 \leq t \leq t_0-1} \cup \{S_{l,t_0}\}_{1 \leq l \leq N_{t_0}}$  and priors selected with domain knowledge. Next, the policymakers choose the trade-off weight  $\omega_{l,t_0}$ , learn a deterministic policy  $\hat{\pi}_{l,t_0}(\cdot; \omega_{l,t_0})$  by planning, and implement  $A_{l,t_0} = \hat{\pi}_{l,t_0}(S_{l,t_0}; \omega_{l,t_0})$ . Formally, we solve the following optimization problem to obtain  $\hat{\pi}_{l,t_0}(\cdot; \omega_{l,t_0})$ :

$$\hat{\pi}_{l,t_0}(\cdot; \omega_{l,t_0}) = \underset{\pi \in \mathcal{F}}{\operatorname{argmin}} \mathbb{E}_{\pi, \rho_{t_0}} \left( \sum_{t=t_0}^T (C_{l,t}^E + \omega_{l,t_0} C_{l,t}^A) \right), \quad (2)$$

where  $\mathbb{E}_{\pi, \rho_{t_0}}$  denotes the expectation assuming  $C_{l,t}^A \sim c_l(A_{l,t})$ ,  $\mathbb{P}(S_{l,t+1} = s_{l,t+1} | S_{l,t} = s_{l,t}, A_{l,t} = a_{l,t}) = f(s_{l,t+1} | s_{l,t}, a_{l,t}; \theta)$  with  $\theta \sim \rho_{t_0}$ , and  $A_{l,t} = \pi(S_{l,t})\mathbb{I}(t \in \mathcal{T}) + A_{l,t-1}\mathbb{I}(t \notin \mathcal{T})$ , for every  $t \geq t_0$ .

The Bayesian approach is preferred because (i) we need to make decisions before accumulating sufficient data, and typically there is important domain knowledge available, and (ii) in this important application, the estimation uncertainty should be taken into consideration in decision-making. The specification of  $\mathcal{F}$  and the policy search algorithms for solving (2) will be discussed in Section 4.3.

### 3.3 Multiple objectives and Pareto-optimal policies

In the discussion above, we assume the tradeoff weight  $\omega_{l,t_0}$  is easily specified at each decision point  $t_0$ . This is feasible when the two objectives share the same unit, for example, when  $C_{l,t}^A$  represents the damage to public health due to economic losses. In general settings, properly choosing the weight is not easy and sometimes unrealistic. Therefore, we aim to assemble a decision support tool that provides a comprehensive picture of the future possibilities associated with different weight choices and hence makes the multi-objective decision-making feasible.

Solving the whole set of Pareto-optimal policies is typically challenging. While in our online planning setting, at each decision point  $t_0$ , we only need to make a one-time decision among a few available actions. For this purpose, it suffices to solve problem (2) for a representative set of weights  $\{\omega_b\}_{b=1}^B$  to find the corresponding Pareto-optimal policies, and then apply Monte Carlo simulation to obtain the corresponding prediction bands for the potential costs following each policy. The policymakers can then compare all these possible options, select among them, and hence choose the action  $A_{l,t_0}$ . With this module, our framework is a *user-in-the-loop* tool. A demo of some information presented to the users is displayed in Figure 3. We summarize this tool in Algorithm 1.

## 4 Details of the Components

### 4.1 State construction

In this section, we discuss the construction of state variables with surveillance data. The data usually available to policymakers is the cumulative count of confirmed cases until time  $t$ , denoted as  $O_{l,t}^I$ . Unlike the infectious disease spread in nature, the individuals counted in  $O_{l,t}^I$  generally either have been confirmed and isolated, or have recovered or died. Therefore, these individuals can be regarded as those removed from the infection system, and it is natural to set  $X_{l,t}^R$  as  $O_{l,t}^I$  (Yang et al., 2020a).

Besides, for infectious diseases, there is typically a time delay between being infectious and getting isolated, the length of which is treated as a random variable with expectation  $D$ . Therefore, the count of the infectious  $X_{l,t}^I$  is usually not immediately observable at time  $t$ , but will be gradually identified in the following days. Following the existing works on infectious disease modelling (Zhang et al., 2005; Chen et al., 2020), we treat this issue as a delayed observation problem and use  $O_{l,t+D}^I - O_{l,t}^I$ , the new confirmed cases during  $(t, t+D]$ , as a proxy for  $X_{l,t}^I$ . In the planning step, following the literature on delayed MDPs (Walsh et al., 2009), we apply Algorithm 2 (Model-based Simulation, MBS) to generate a proxy state, and then choose the action according to it. We note that although this issue is not obvious



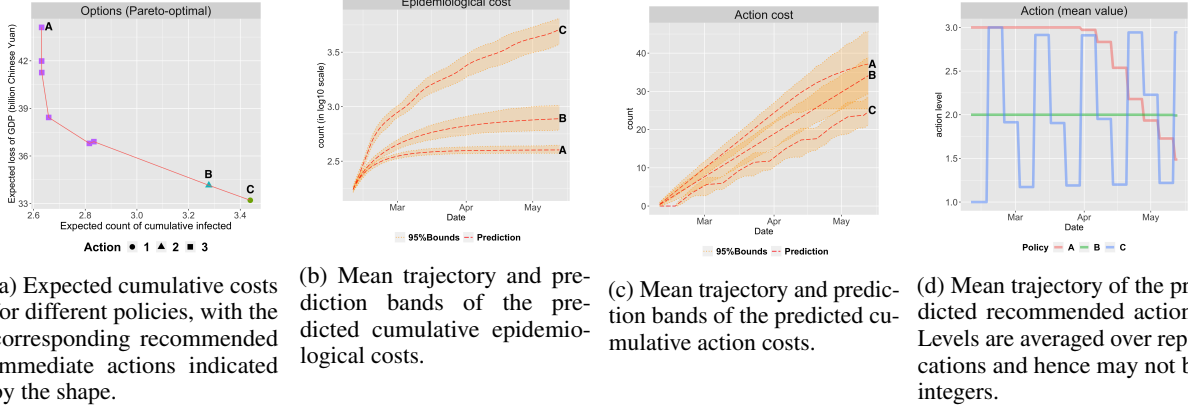


Figure 3: A demo of some information presented to the users. Results are computed for Beijing, China on 02/10/2020. The proposed method is run under the experiment setting introduced in Section 5, where we consider three levels of actions. For three sample policies, we plot the predicted behaviour of them in subplot (b)-(d). Prediction results are aggregated over 1000 replications. According to subplot (d), policies A and B can be interpreted as the suppression and mitigation policy studied in (Ferguson et al., 2020), and policy C is close to the periodic lockdown policy suggested in the literature (Bin et al., 2020; Karin et al., [n.d.]).

---

#### Algorithm 1: Pareto-optimal Policies and Prediction Bands

---

**Input:** weights  $\{\omega_b\}_{b=1}^B$ , number of replications  $K$ , significance level  $\alpha$ , action cost function  $c_l(\cdot)$ , decision points  $\mathcal{T}, \mathcal{D}_{t_0}, \rho_{t_0}, T$ .

**for**  $b = 1, \dots, B$  **do**

    apply a policy search algorithm to find the optimal policy  $\hat{\pi}^b$  for weight  $\omega_b$ .

**for**  $k = 1, \dots, K$  **do**

        set the cumulative cost  $V_{t_0-1}^{k,E}$  and  $V_{t_0-1}^{k,A}$  as 0

        set  $S_{t_0,b}^k = S_{t_0}$

**for**  $t = t_0, \dots, T$  **do**

            choose action  $A_{t,b}^k = \hat{\pi}^b(S_{t,b}^k)\mathbb{I}(t \in \mathcal{T}) + A_{t-1,b}^k\mathbb{I}(t \notin \mathcal{T})$

            sample  $C_{t,b}^{k,A} \sim c_l(A_{t,b}^k)$ ,  $\theta_{t,b}^k \sim \rho_{t_0}$ , and  $S_{t+1,b}^k \sim f(\cdot | S_{t,b}^k, A_{t,b}^k; \theta_{t,b}^k)$

            calculate  $V_{t,b}^{k,E} = V_{t-1,b}^{k,E} + X_{t,b}^{k,S} - X_{t+1,b}^{k,S}$  and  $V_{t,b}^{k,A} = V_{t-1,b}^{k,A} + C_{t,b}^{k,A}$

        for every  $t$ , calculate the upper and lower  $\alpha/2$ -th quantile and the mean of  $\{V_{t,b}^{k,E}\}_{k=1}^K$  as  $V_{u,t}^{b,E}, V_{l,t}^{b,E}$ , and  $\bar{V}_t^{b,E}$ , respectively; similarly calculate  $V_{u,t}^{b,A}, V_{l,t}^{b,A}$ , and  $\bar{V}_t^{b,A}$ .

**Result:** optimal policies  $\{\hat{\pi}^b\}_{b=1}^B$ , recommended actions  $\{A_{t_0,b}^1\}_{b=1}^B$ , prediction bands for costs

$$\left\{ \left\{ (V_{l,t}^{b,E}, V_{u,t}^{b,E}, \bar{V}_t^{b,E}), (V_{l,t}^{b,A}, V_{u,t}^{b,A}, \bar{V}_t^{b,A}) \right\}_{t=t_0}^T \right\}_{b=1}^B$$


---

in prediction, it is unavoidable in decision-making because  $A_{l,t}$  works directly on  $X_{l,t}^I$ . The performance of such an approximation is supported by the theoretical analysis in (Walsh et al., 2009) and the experiments in Section 5.

## 4.2 Estimation of the transition model

At each time  $t_0 \in \mathcal{T}$ , we need to first obtain the posterior of  $\theta$  in the transition model (1). Notice that the last equation in (1) is redundant under the constraint  $X_{l,t}^S + X_{l,t}^I + X_{l,t}^R = M_l$  for all  $t$ . With data  $\mathcal{D}_{t_0}$ , the Markov property reduces the estimation problem to  $J + 1$  Bayesian generalized linear models with the identity link function. By choosing the priors as the conjugate priors, the posterior distributions have explicit forms. Specifically, let  $\gamma \sim \text{Beta}(a_R, b_R)$  with parameters  $(a_R, b_R)$ , and let  $\beta_j \sim \text{Beta}(a_{S,j}, b_{S,j})$  with parameters  $(a_{S,j}, b_{S,j})$ , for  $j = 1, \dots, J$ . Under the assumption that these priors are independent, we have  $\gamma | \mathcal{D}_{t_0} \sim \text{Beta}(a_R^*, b_R^*)$  and  $\beta_j | \mathcal{D}_{t_0} \sim \text{Gamma}(a_{S,j}^*, b_{S,j}^*)$ ,

**Algorithm 2:** Model-based Simulation (MBS)

**Data:**  $\{O_{l,t}^I\}_{t=t_0-D}^{t_0}$ ,  $\{A_{l,t}\}_{t=t_0-D}^{t_0-1}$ ,  $\rho_{t_0}$ , and  $D$ 

 set  $X_{l,t_0-D}^{I,G} = O_{l,t_0}^I - O_{l,t_0-D}^I$  and  $(\hat{\gamma}_{t_0}, \hat{\beta}_{1,t_0}, \dots, \hat{\beta}_{J,t_0})^T = \mathbb{E}(\rho_{t_0})$ .

**for**  $t = t_0 - D, \dots, t_0 - 1$  **do**

$$\left[ X_{l,t+1}^{I,G} = X_{l,t}^{I,G} + \sum_{j=1}^J \hat{\beta}_{j,t_0} \mathbb{I}_{\{A_{l,t}=j\}} (M_l - O_{l,t}^I - X_{l,t}^{I,G}) X_{l,t}^{I,G} / M_l - (O_{l,t+1}^I - O_{l,t}^I) \right]$$
**Result:** the proxy state  $S_{l,t_0} = (M_l - X_{l,t_0}^{I,G} - O_{l,t_0}^I, X_{l,t_0}^{I,G}, O_{l,t_0}^I)^T$ 

 for  $j = 1, \dots, J$ , where

$$\begin{aligned} a_{S,j}^* &= a_{S,j} + \sum_{(t,l) \in \Omega_{t_0,j}} (X_{l,t}^S - X_{l,t+1}^S), \quad b_{S,j}^* = b_{S,j} + \sum_{(t,l) \in \Omega_{t_0,j}} \frac{X_{l,t}^S X_{l,t+1}^I}{M_l}, \\ a_R^* &= a_R + \sum_{(t,l) \in \Omega_{t_0}} (X_{l,t+1}^R - X_{l,t}^R), \quad b_R^* = b_R - \sum_{(t,l) \in \Omega_{t_0}} (X_{l,t+1}^R - X_{l,t}^R) + \sum_{(t,l) \in \Omega_{t_0}} X_{l,t}^I, \end{aligned}$$

 where  $\Omega_{t_0,j} = \{(t,l) : 1 \leq t \leq t_0 - 1, 1 \leq l \leq N_t, A_{l,t} = j\}$  is the set of time-location pairs where action  $j$  is taken, and  $\Omega_{t_0} = \bigcup_j \Omega_{t_0,j}$ .

Below, we introduce a way to specify the prior parameters: (i)  $\beta_1$  and  $\gamma$  are both features of this disease without any interventions, and we can first set their priors with the estimates of similar diseases, and update them when additional biochemical findings are available; (ii) for  $j \geq 2$ ,  $\beta_j$  indicates the infection rate under action level  $j$ . Suppose we have a reasonable estimate of the intervention effect  $u_j = \beta_j / \beta_1$  as  $\hat{u}_j$  and that of  $\beta_1$  as  $\hat{\beta}_1$ , then the prior of  $\beta_j$  can be set as a distribution with expectation  $\hat{u}_j \hat{\beta}_1$ .

### 4.3 Policy search

At each decision point  $t_0 \in \mathcal{T}$ , for each region  $l$  and a given weight  $\omega_{l,t_0}$ , we need to learn the optimal policy  $\hat{\pi}_{l,t_0}(\cdot; \omega_{l,t_0}) \in \mathcal{F}$  by solving the model-based planning problem (2). We introduce two types of policy classes and the corresponding planning algorithms, with emphasis on either the interpretability or the global optimality.

**Interpretable policy class.** In applications of infectious disease control, the interpretability of the policy is typically important. In this case, we need to restrict our attention to an interpretable parametric policy class. As an illustration, in this work, we consider the following observations from the pandemic control decision-making process in real life: (i) the decision should be based on the spread severity, which we interpret as  $X_{l,t}^I$ , the number of infectious individuals; (ii) the policy should also be based on the current estimate of disease features  $\rho_{t_0}$ , the current state  $S_{l,t_0}$ , the trade-off weight  $\omega_{l,t_0}$ , and the potential cost  $c_l(\cdot)$ , which have all been incorporated in the objective function of (2); (iii) the more serious the situation, the more stringent the intervention should be. Motivated by these observations, we focus on the threshold-based policy class:

$$\begin{aligned} \mathcal{F} &= \{\pi : \pi(S_{l,t}; \boldsymbol{\lambda}) = \sum_{j=1}^J j \mathbb{I}(\lambda_j \leq X_{l,t}^I < \lambda_{j+1}), \\ &0 = \lambda_1 \leq \lambda_2 \leq \dots \leq \lambda_{J+1} = M_l, \lambda_J \leq \lambda_M\}, \end{aligned} \quad (3)$$

where  $\boldsymbol{\lambda} = (\lambda_2, \dots, \lambda_J)^T$ . Notice that  $X_{l,t}^I$  is generally a number much smaller than the population  $M_l$ , we introduce the pre-specified tolerance parameter  $\lambda_M \in (0, M_l)$  to reduce the computational cost by deleting unrealistic policies.

Given a specified policy class, problem (2) can be then solved via rollout-based direct policy search. Direct policy search algorithms (Gosavi et al., 2015) generally apply optimization algorithms to maximize the value function approximated via Monte Carlo rollouts. For class (3), since the state transition and the action cost are both computationally affordable to sample, when  $J$  is not large, we can simply apply the grid search algorithm, which is robust and safe in such an important application. The example for  $J = 3$ , which is the case in our experiment, is described in Algorithm 3 in Appendix A. When  $J$  is large, many other optimization algorithms such as the simultaneous perturbation stochastic approximation algorithm (Sadegh, 1997) can be used. Alternatively, one can apply the deterministic policy gradient (Silver et al., 2014) or actor-critic (Lillicrap et al., 2015) with the learned environment model as a simulator.

Table 1: Posterior means and standard deviations (in the parentheses) obtained using data for all the six cities until day  $t_0$ .

$t_0$	$R_0^1$	$R_0^2$	$R_0^3$	$\gamma$	$\beta_1$	$\beta_2$	$\beta_3$
12	4.13 (.34)	0.74 (.09)	0.37 (.06)	0.07 (.005)	0.29 (.011)	0.05 (.005)	0.03 (.004)
61	2.32 (.09)	0.70 (.03)	0.38 (.03)	0.11 (.002)	0.25 (.007)	0.07 (.003)	0.04 (.003)

**Black-box policy class.** If the interpretability can be traded off for global optimality, a more complex policy class can be considered. Since the action set is discrete, multiple planning algorithms in the literature are applicable, such as Monte carlo tree search with state aggregation (Hostetler et al., 2014). As an example, in this work, we focus on the policy class  $\mathcal{F}$  induced by a class of deep-Q value network (DQN) (Mnih et al., 2015) with an augmented state space  $\mathcal{S} \times \{1, 2, \dots, T\}$ . Specifically, to take into consideration the learned model uncertainty  $\rho_{t_0}$ , we define the Q-function of policy  $\pi$  as  $Q_{l,t_0}^\pi((s, t'), a; \omega_{l,t_0}) = \mathbb{E}_{\pi, \rho_{t_0}}(\sum_{t=t'}^T (C_{l,t}^E + \omega_{l,t_0} C_{l,t}^A))$ , and then apply value iteration with epsilon-greedy exploration to learn the optimal value function as  $\hat{Q}_{l,t_0}^*(\cdot, \cdot; \omega_{l,t_0})$ . The corresponding policy is the induced greedy policy. More details can be found in Appendix A.

## 5 Experiments

In this section, we apply our framework to some COVID-19 data in China for illustration. China has passed the first peak, which provides data of good quality for validation purposes. To further investigate the applicability of our framework to other diseases and its robustness, we also run an experiment with parameters of the 2009 H1N1 pandemic and conduct several sensitivity analysis.

### 5.1 Data description and hyper-parameters

We collect data for six important cities in China from 01/15/2020 to 05/13/2020, and index these cities by  $l \in \{1, \dots, 6\}$  and dates by  $t \in \{1, \dots, 120\}$ , with  $T = 120$ . More details about the dataset, data sources, and hyper-parameters can be found in Appendix C.1.

**State variables and region-specific features:** For each region  $l$ , we collect its annual gross domestic product (GDP)  $G_l$ , population  $M_l$ , and counts of confirmed cases from official sources.

**Action:** three levels of interventions implemented in China during COVID-19 are considered: level 1 means no or few official policies claimed; level 2 means the public health emergency response; level 3 means the stringent closed-off management required by the government. Data are collected from the news.

**Cost:** we use  $r_{l,t}$ , the observed ratio of human mobility loss in city  $l$  on day  $t$  compared with year 2019, to construct a proxy for its GDP loss and calibrate the action cost function  $c_l(\cdot)$ . For  $j \in \{2, 3\}$ , we first fit a normal distribution  $\mathcal{N}(\mu_j, \sigma_j^2)$  to the observed loss ratios under the corresponding intervention level. We then define  $c_l(a)$  as  $\sum_{j=1}^3 C_j \mathbb{I}(a = j) G_l / 365$ , where  $C_1 = 0$  and  $C_j \sim \mathcal{N}(\mu_j, \sigma_j^2)$  for  $j \in \{2, 3\}$ . We note that this is only for illustration purposes. In real applications, policymakers need to carefully design and measure the potential costs with domain experts.

**Hyper-parameters:** the parameter estimates for a similar pandemic SARS (Mkhatshwa and Mummert, 2010) are used as priors of  $\gamma$  and  $\beta_1$ . Similar to (Ferguson et al., 2020), we assume that action 2 and 3 can reduce the infection rate by 80% and 90%, respectively, and set the priors for  $\beta_2$  and  $\beta_3$  accordingly.  $D$  is chosen as 9 according to (Sun et al., 2020) and (Pellis et al., 2020).

### 5.2 Estimation and validation of the transition model

The performance of our learned policies and the choices of weights both rely on the prediction accuracy of the estimated GSIR model, and we aim to first examine this point via temporal validation. Specifically, we first estimate the GSIR model using all data until day 12, and then for each city  $l$ , we predict  $X_{l,t}^R$ , the count of cumulative confirmed cases, from day 13 to 120 following the observed actions in data via forward sampling with the estimated GSIR model. Such a prediction can partially reflect the quality of our decisions suppose when we are on day 12. The results aggregated over 1000 replications are plotted in Figure 4 and the prediction bands successfully cover the observed counts in most cases.

To provide more insights into the intervention effects, in Table 1, we present the estimated parameters using all data until day 61, since the new cases afterwards are sparse. Here,  $R_0^j = \beta_j / \gamma$  is the basic reproduction number under action level



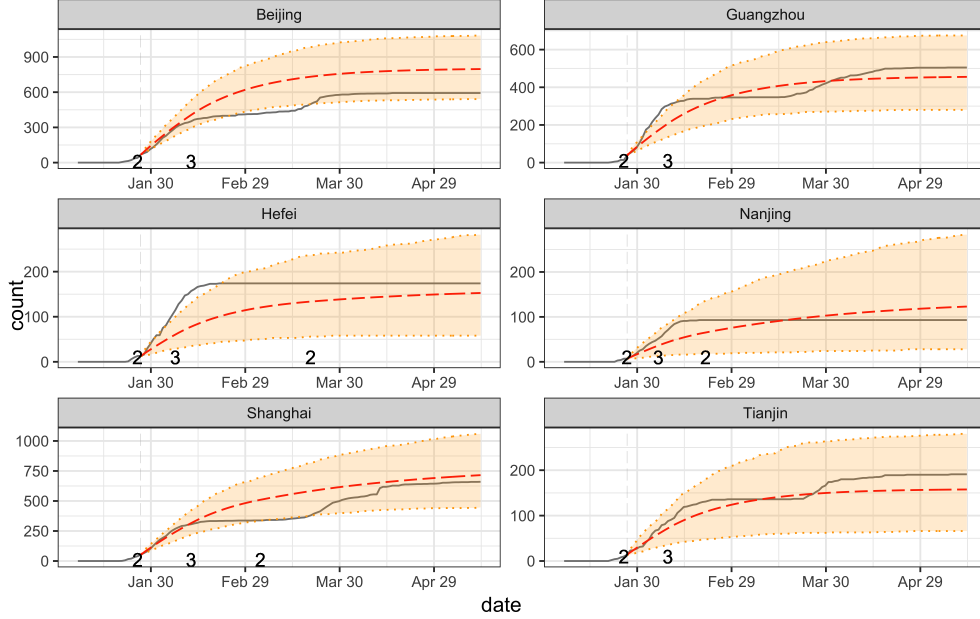


Figure 4: Validation results for the six important cities in China. The solid lines are the observed counts of the cumulative infected cases. The red dotted lines represent the mean predicted numbers, with the shaded areas indicating the 99% prediction bands. When a different action was taken, we annotate the new action level on the change point.

$j$ , which plays an essential role in epidemiology analysis (Delamater et al., 2019). Roughly speaking,  $R_0^j < 1$  implies the pandemic will gradually diminish under action  $j$ . The small value of  $R_0^3$  indicates that action 3 has a significant effect on controlling the pandemic; measure 2 is also effective and is more like a mitigation strategy; the value of  $R_0^1$  emphasizes that a lack of intervention will lead to a disaster. The estimates of  $R_0^1$  and intervention effects ( $R_0^2/R_0^1$  and  $R_0^3/R_0^1$ ) are consistent with the existing results surveyed in (Alimohamadi et al., 2020) and (Cheatley et al., 2020). We also reported the estimates used to make the predictions in Figure 4. Although the estimation is not perfect due to data scarcity in the early stage, the prediction still captures the rough trend under a reasonable policy and we expect it will not affect the decision-making significantly.

### 5.3 Evaluation of the Pareto-optimal policies

In this section, we conduct simulation experiments to compare the performance of our proposed method with several competing policies on curbing the spread of COVID-19. Specifically, for the six cities, we start from day 12 together, and follow the actions recommended by a specific policy until day 120, with the cumulative costs recorded. The state transitions are generated from the GSIR model with  $\mathbb{E}(\rho_{61})$  as the parameter, and the observations before day 12 are kept the same with the real data. This design is to mimic a real infectious disease control following some specified policy or algorithm. Although this is a simulation study, we still investigated the validity of  $\mathbb{E}(\rho_{61})$  as the environment parameter for fair comparison with the observed costs in the real data. Its validity is supported by the cross-validation results in Appendix C.3. It also partially supports that these regions are similar.

We compare our algorithm with several expert policies that are motivated by real life observations and commonly considered in the literature (Merl et al., 2009; Lin et al., 2010; Ludkovski and Niemi, 2010). Specifically, the comparisons are made among the following policies:

1. Our proposed Pareto-optimal policies  $\pi_k$  for  $k \in \{-2, 0, \dots, 6\}$ : we fix the weight as  $e^k/10$  across all cities and time, and follow the workflow proposed in Section 3.2.  $\mathcal{T}$  is set as every seven days. We consider both the threshold-based policy class (3) and the DQN-based method.
2. Occurrence-based mitigation policy  $\pi_m^M$  for  $m \in \{4, 6, \dots, 12\}$ : a city implements action 2 when there are new cases confirmed in the past  $m$  days, and action 1 otherwise.
3. Occurrence-based suppression policy  $\pi_m^S$  for  $m \in \{4, 6, \dots, 10\}$ : a city begins to implement action 2 after  $m$  days from its first confirmed case and strengthens it to level 3 after  $m$  more days. Afterwards, the city weakens

the action to level 2 when there have been no new cases for  $m$  days and level 1 there have been no new cases for  $2m$  days.

4. Count threshold-based policy  $\pi_m^{TB}$  for  $m \in \{5, 10, \dots, 50\}$ : a city implements action 3 when the count of new cases on the day before exceeds  $m$ , action 1 when it is zero, and action 2 otherwise.
5. Behaviour policy  $\pi^B$ : the observed trajectories in the dataset.

For each policy except for  $\pi^B$ , we run 100 replications and present the average costs in Figure 5. We can see that the proposed method provides a clear view of the tradeoff and its performance is generally better than the competing policies. In some cases, the DQN-based policies are slightly better than the threshold-based policies, while the overall value difference is not large. The behaviour policy by Chinese local governments is quite strict in the later period, and we interpret part of this effort as the attempt to curb the cross-border spread. The other policies are not Pareto-optimal and also are not adaptive to different situations in different cities. The clear trend among the occurrence-based suppression policies emphasizes the importance of intervening as promptly as possible, which can reduce both costs.

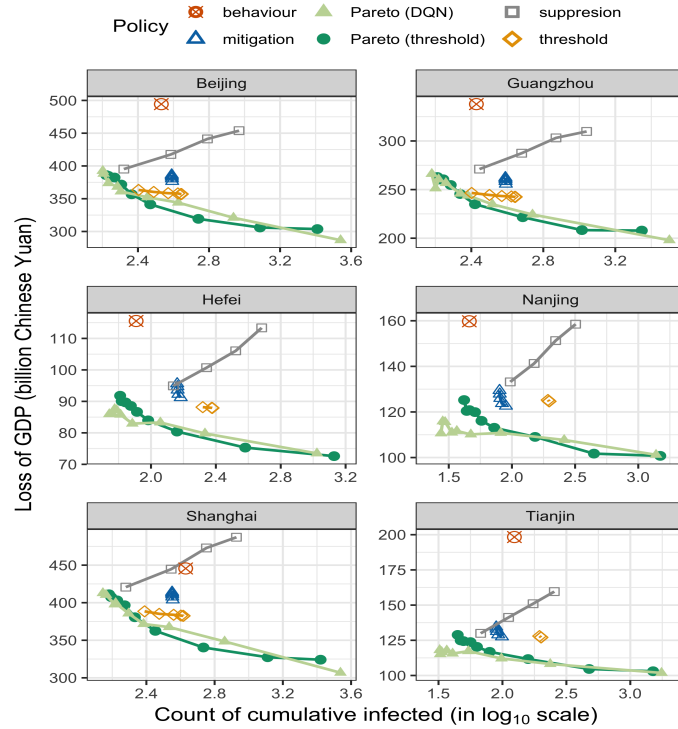


Figure 5: Cumulative epidemiological costs and economic costs following different policies, averaged over 100 replications. The closer to the left bottom corner, the better. The standard errors are negligible. On each curve, the different markers represent the performance of a policy with different hyper-parameters.

To further investigate the robustness of the proposed method, two sensitivity analyses are conducted. Specifically, we repeat the above experiment with either various combinations of hyper-parameters or with the data generation model modified as a generalized Susceptible-Exposed-Infected-Removal model (Tang et al., 2020). The results can be found in Appendix B. In reasonable ranges, the proposed method still yields consistent and superior performance.

Finally, recall that infectious disease control is about trade-off. For a disease as infectious as the COVID-19, usually a stricter policy would be preferred. However, for a less infectious one, the same response policy might result in over-reaction and hence unnecessary costs to the economics. To demonstrate the adaptiveness of the proposed method, we repeat the above experiment with a less infectious disease. Specifically, we calibrate the GSIR model with the parameters of the 2009 H1N1 pandemic, with the other settings kept the same for ease of comparison. We choose the parameters estimated in (Fraser et al., 2009), which reports an  $R_0$  of about 1.4.

The results are summarized in Figure 6. We can see that the proposed method still yields superior performance. The count threshold-based policies achieve close performance with some Pareto-optimal policies, while our method provides more options with a clear trade-off. Compared to Figure 5, the economic costs of the strict suppression policy increase, relative to the other policies.

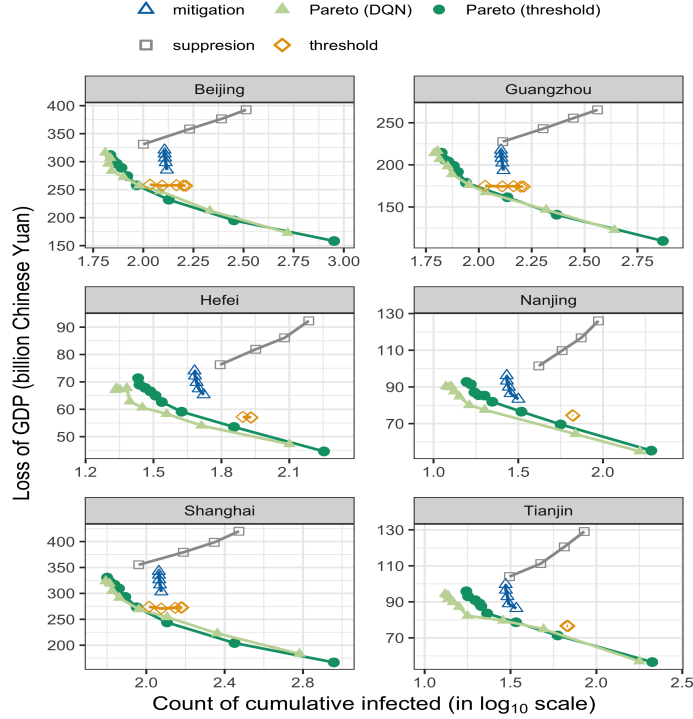


Figure 6: Experiment results with model parameters calibrated from the H1N1 pandemic. The costs of the behaviour policy are not displayed since they are not comparable.

## 6 Discussion

Motivated by the ongoing COVID-19 pandemic and the witnessed challenges in decision-making for policymakers, this paper proposes a novel model-based multi-objective RL framework to assist policymakers in real-time decision-making with the objective of minimizing the overall long-term cost. The method shows promising performance in numerical studies.

The overall framework is generally applicable to infectious disease pandemics. There are several components that can be extended: (i) other epidemiology models than the SIR model can also be used as the transition model, with the estimation method and policy class modified correspondingly; (ii) more than two objectives can be similarly formalized, and resource limits can also be considered by introducing a cost to penalize exceeding the limits; (iii) other parametric policy classes can be similarly formalized depending on the information required for decision-making.

We note that modeling the economic costs caused by various intervention measures is, admittedly, a challenging but important task. This is out of the scope of this paper and we use a simple proxy in the experiment for illustration purposes. A systematic analysis of the observed costs during COVID-19 would be a meaningful next step. Besides, choosing among the Pareto-optimal policies is another challenging task, which is arguably beyond the scope of data-driven methods. Options can be presented to a committee or the citizens for discussion or voting.

As future directions, the spreads among multiple regions can be incorporated under the multi-agent RL framework, the heterogeneity of different regions can be accounted in a similar way as in (Qian et al., 2020) if we have enough data, and a multidimensional action space with the combinations of different interventions can be considered.

Finally, we would like to emphasize that taking the economy as more important than human lives is not a motivation or an outcome of this framework. On one hand, economic losses can also cause health damage to many people, probably no less than the direct damage from the disease; on the other hand, the estimated Pareto-optimal policies aim to help policymakers reduce the cost on one objective without sacrificing the other, as illustrated in Section 5.3.

## References

Yousef Alimohamadi, Maryam Taghdir, and Mojtaba Sepandi. 2020. The estimate of the basic reproduction number for novel coronavirus disease (COVID-19): a systematic review and meta-analysis. *Journal of Preventive Medicine and*

- Public Health* (2020).
- Fernando E Alvarez, David Argente, and Francesco Lippi. 2020. *A simple planning problem for covid-19 lockdown*. Technical Report. National Bureau of Economic Research.
- Roy M Anderson, Hans Heesterbeek, Don Klinkenberg, and T Déirdre Hollingsworth. 2020. How will country-based mitigation measures influence the course of the COVID-19 epidemic? *The Lancet* 395, 10228 (2020), 931–934.
- Raghav Awasthi, Keerat Kaur Guliani, Arshita Bhatt, Mehrab Singh Gill, Aditya Nagori, Ponnurangam Kumaraguru, and Tavpritesh Sethi. 2020. VacSIM: Learning Effective Strategies for COVID-19 Vaccine Distribution using Reinforcement Learning. *arXiv preprint arXiv:2009.06602* (2020).
- Leon Barrett and Sridhar Narayanan. 2008. Learning all optimal policies with multiple criteria. In *Proceedings of the 25th international conference on Machine learning*. 41–47.
- M Bin, P Cheung, E Crisostomi, P Ferraro, H Lhachemi, R Murray-Smith, C Myant, T Parisini, R Shorten, S Stein, et al. 2020. Post-lockdown abatement of COVID-19 by fast periodic switching. *arXiv: 2003.09930* (2020).
- Fred Brauer. 2008. Compartmental models in epidemiology. In *Mathematical epidemiology*. Springer, 19–79.
- Cameron B Browne, Edward Powley, Daniel Whitehouse, Simon M Lucas, Peter I Cowling, Philipp Rohlfshagen, Stephen Tavener, Diego Perez, Spyridon Samothrakis, and Simon Colton. 2012. A survey of monte carlo tree search methods. *IEEE Transactions on Computational Intelligence and AI in games* 4, 1 (2012), 1–43.
- Andrea Castelletti, Francesca Pianosi, and Marcello Restelli. 2012. Tree-based fitted Q-iteration for multi-objective Markov decision problems. In *The 2012 International Joint Conference on Neural Networks (IJCNN)*. IEEE, 1–8.
- Jane Cheatley, Sabine Vuik, Marion Devaux, Stefano Scarpetta, Mark Pearson, Francesca Colombo, and Michele Cecchini. 2020. The effectiveness of non-pharmaceutical interventions in containing epidemics: a rapid review of the literature and quantitative assessment. *medRxiv* (2020).
- Baoquan Chen, Mingyi Shi, Xingyu Ni, Liangwang Ruan, Hongda Jiang, Heyuan Yao, Mengdi Wang, Zhenghua Song, Qiang Zhou, and Tong Ge. 2020. Data Visualization Analysis and Simulation Prediction for COVID-19. *arXiv preprint arXiv:2002.07096* (2020).
- Paul L Delamater, Erica J Street, Timothy F Leslie, Y Tony Yang, and Kathryn H Jacobsen. 2019. Complexity of the basic reproduction number (R0). *Emerging infectious diseases* 25, 1 (2019), 1.
- Hamid Eftekhari, Debarghya Mukherjee, Moulinath Banerjee, and Ya’acov Ritov. 2020. Markovian And Non-Markovian Processes with Active Decision Making Strategies For Addressing The COVID-19 Epidemic. *arXiv preprint arXiv:2008.00375* (2020).
- Martin S Eichenbaum, Sergio Rebelo, and Mathias Trabandt. 2020. *The macroeconomics of epidemics*. Technical Report. National Bureau of Economic Research.
- Mohamed Elhia, Mostafa Rachik, and Elhabib Benlahmar. 2013. Optimal control of an SIR model with delay in state and control variables. *ISRN Biomathematics* 2013 (2013).
- Vladimir Feinberg, Alvin Wan, Ion Stoica, Michael I Jordan, Joseph E Gonzalez, and Sergey Levine. 2018. Model-based value estimation for efficient model-free reinforcement learning. *arXiv preprint arXiv:1803.00101* (2018).
- NM Ferguson, D Laydon, G Nedjati-Gilani, et al. 2020. Impact of non-pharmaceutical interventions (NPIs) to reduce COVID-19 mortality and healthcare demand. Imperial College COVID-19 Response Team.
- Christophe Fraser, Christl A Donnelly, Simon Cauchemez, William P Hanage, Maria D Van Kerkhove, T Déirdre Hollingsworth, Jamie Griffin, Rebecca F Baggaley, Helen E Jenkins, Emily J Lyons, et al. 2009. Pandemic potential of a strain of influenza A (H1N1): early findings. *science* 324, 5934 (2009), 1557–1561.
- Anuj Gangopadhyaya and A Bowen Garrett. 2020. Unemployment, Health Insurance, and the COVID-19 Recession. *Health Insurance, and the COVID-19 Recession (April 1, 2020)* (2020).
- Abhijit Gosavi et al. 2015. *Simulation-based optimization*. Springer.
- Leonhard Held, Niel Hens, Philip D O’Neill, and Jacco Wallinga. 2019. *Handbook of infectious disease data analysis*. CRC Press.
- Joel Hellewell, Sam Abbott, Amy Gimma, Nikos I Bosse, Christopher I Jarvis, Timothy W Russell, James D Munday, Adam J Kucharski, W John Edmunds, Fiona Sun, et al. 2020. Feasibility of controlling COVID-19 outbreaks by isolation of cases and contacts. *The Lancet Global Health* (2020).
- Jesse Hostetler, Alan Fern, and Tom Dietterich. 2014. State aggregation in Monte Carlo tree search. In *Proceedings of the AAAI Conference on Artificial Intelligence*, Vol. 28.

- Omer Karin, Yinon M Bar-On, Tomer Milo, Itay Katzir, Avi Mayo, Yael Korem, Boaz Dudovich, Eran Yashiv, Amos J Zehavi, Nadav Davidovitch, et al. [n.d.]. Cyclic exit strategies to suppress COVID-19 and allow economic activity. ([n. d.]).
- Matt J Keeling and Pejman Rohani. 2011. *Modeling infectious diseases in humans and animals*. Princeton University Press.
- William Ogilvy Kermack and Anderson G McKendrick. 1927. A contribution to the mathematical theory of epidemics. *Proceedings of the royal society of london. Series A, Containing papers of a mathematical and physical character* 115, 772 (1927), 700–721.
- Vijay R Konda and John N Tsitsiklis. 2000. Actor-critic algorithms. In *Advances in neural information processing systems*. 1008–1014.
- Hannah M Korevaar, Alexander David Becker, Ian F Miller, Bryan T Grenfell, C Jessica E Metcalf, and Michael J Mina. 2020. Quantifying the impact of US state non-pharmaceutical interventions on COVID-19 transmission. *medRxiv* (2020).
- China Data Lab. 2020. China COVID-19 Daily Cases with Basemap. <https://doi.org/10.7910/DVN/MR5IJN>
- Eric B Laber, Nick J Meyer, Brian J Reich, Krishna Pacifici, Jaime A Collazo, and John M Drake. 2018. Optimal treatment allocations in space and time for on-line control of an emerging infectious disease. *Journal of the Royal Statistical Society: Series C (Applied Statistics)* 67, 4 (2018), 743–789.
- Urszula Ledzewicz and Heinz Schättler. 2011. On optimal singular controls for a general SIR-model with vaccination and treatment. *Discrete and continuous dynamical systems 2* (2011), 981–990.
- Timothy P Lillicrap, Jonathan J Hunt, Alexander Pritzel, Nicolas Heess, Tom Erez, Yuval Tassa, David Silver, and Daan Wierstra. 2015. Continuous control with deep reinforcement learning. *arXiv preprint arXiv:1509.02971* (2015).
- Feng Lin, Kumar Muthuraman, and Mark Lawley. 2010. An optimal control theory approach to non-pharmaceutical interventions. *BMC infectious diseases* 10, 1 (2010), 32.
- Chunming Liu, Xin Xu, and Dewen Hu. 2014. Multiobjective reinforcement learning: A comprehensive overview. *IEEE Transactions on Systems, Man, and Cybernetics: Systems* 45, 3 (2014), 385–398.
- Michael Ludkovski and Jarad Niemi. 2010. Optimal dynamic policies for influenza management. *Statistical Communications in Infectious Diseases* 2, 1 (2010).
- Daniel Merl, Leah R Johnson, Robert B Gramacy, and Marc Mangel. 2009. A statistical framework for the adaptive management of epidemiological interventions. *PLoS One* 4, 6 (2009), e5807.
- Thembinkosi Mkhathshwa and Anna Mummert. 2010. Modeling super-spreading events for infectious diseases: case study SARS. *arXiv preprint arXiv:1007.0908* (2010).
- Volodymyr Mnih, Koray Kavukcuoglu, David Silver, Andrei A Rusu, Joel Veness, Marc G Bellemare, Alex Graves, Martin Riedmiller, Andreas K Fidjeland, Georg Ostrovski, et al. 2015. Human-level control through deep reinforcement learning. *Nature* 518, 7540 (2015), 529–533.
- Sriraam Natarajan and Prasad Tadepalli. 2005. Dynamic preferences in multi-criteria reinforcement learning. In *Proceedings of the 22nd international conference on Machine learning*. 601–608.
- World Health Organization et al. 2020. Coronavirus disease 2019 (COVID-19): situation report, 72. (2020).
- Simone Parisi, Matteo Pirotta, and Jan Peters. 2017. Manifold-based multi-objective policy search with sample reuse. *Neurocomputing* 263 (2017), 3–14.
- Lorenzo Pellis, Francesca Scarabel, Helena B Stage, Christopher E Overton, Lauren HK Chappell, Katrina A Lythgoe, Elizabeth Fearon, Emma Bennett, Jacob Curran-Sebastian, Rajenki Das, et al. 2020. Challenges in control of Covid-19: short doubling time and long delay to effect of interventions. *arXiv preprint arXiv:2004.00117* (2020).
- Facundo Pigullem and Liyan Shi. 2020. Optimal COVID-19 quarantine and testing policies. (2020).
- Matteo Pirotta, Simone Parisi, and Marcello Restelli. 2015. Multi-objective reinforcement learning with continuous pareto frontier approximation. In *Twenty-Ninth AAAI Conference on Artificial Intelligence*.
- William JM Probert, Chris P Jewell, Marleen Werkman, Christopher J Fonnesebeck, Yoshitaka Goto, Michael C Runge, Satoshi Sekiguchi, Katriona Shea, Matt J Keeling, Matthew J Ferrari, et al. 2018. Real-time decision-making during emergency disease outbreaks. *PLoS computational biology* 14, 7 (2018), e1006202.
- Martin L Puterman. 2014. *Markov decision processes: discrete stochastic dynamic programming*. John Wiley & Sons.
- Zhaozhi Qian, Ahmed M Alaa, and Mihaela van der Schaar. 2020. When to Lift the Lockdown? Global COVID-19 Scenario Planning and Policy Effects using Compartmental Gaussian Processes. *arXiv preprint arXiv:2005.08837* (2020).



- Martin Riedmiller. 2005. Neural fitted Q iteration—first experiences with a data efficient neural reinforcement learning method. In *European Conference on Machine Learning*. Springer, 317–328.
- Weston C Roda, Marie B Varughese, Donglin Han, and Michael Y Li. 2020. Why is it difficult to accurately predict the COVID-19 epidemic? *Infectious Disease Modelling* (2020).
- Diederik M Roijers, Peter Vamplew, Shimon Whiteson, and Richard Dazeley. 2013. A survey of multi-objective sequential decision-making. *Journal of Artificial Intelligence Research* 48 (2013), 67–113.
- Payman Sadegh. 1997. Constrained optimization via stochastic approximation with a simultaneous perturbation gradient approximation. *Automatica* 33, 5 (1997), 889–892.
- David Silver, Guy Lever, Nicolas Heess, Thomas Degris, Daan Wierstra, and Martin Riedmiller. 2014. Deterministic policy gradient algorithms. In *International conference on machine learning*. PMLR, 387–395.
- Peter X Song, Lili Wang, Yiwang Zhou, Jie He, Bin Zhu, Fei Wang, Lu Tang, and Marisa Eisenberg. 2020a. An epidemiological forecast model and software assessing interventions on COVID-19 epidemic in China. *medRxiv* (2020).
- Sirui Song, Zefang Zong, Yong Li, Xue Liu, and Yang Yu. 2020b. Reinforced Epidemic Control: Saving Both Lives and Economy. *arXiv preprint arXiv:2008.01257* (2020).
- Haoxuan Sun, Yumou Qiu, Han Yan, Yaxuan Huang, Yuru Zhu, and Song Xi Chen. 2020. Tracking and Predicting COVID-19 Epidemic in China Mainland. *medRxiv* (2020).
- Richard S Sutton and Andrew G Barto. 2018. *Reinforcement learning: An introduction*. MIT press.
- Lu Tang, Yiwang Zhou, Lili Wang, Soumik Purkayastha, Leyao Zhang, Jie He, Fei Wang, and Peter X-K Song. 2020. A Review of Multi-Compartment Infectious Disease Models. *International Statistical Review* 88, 2 (2020), 462–513.
- Michael J Tildesley, Nicholas J Savill, Darren J Shaw, Rob Deardon, Stephen P Brooks, Mark EJ Woolhouse, Bryan T Grenfell, and Matt J Keeling. 2006. Optimal reactive vaccination strategies for a foot-and-mouth outbreak in the UK. *Nature* 440, 7080 (2006), 83–86.
- Hado P van Hasselt, Matteo Hessel, and John Aslanides. 2019. When to use parametric models in reinforcement learning?. In *Advances in Neural Information Processing Systems*. 14322–14333.
- Kristof Van Moffaert, Madalina M Drugan, and Ann Nowé. 2013. Scalarized multi-objective reinforcement learning: Novel design techniques. In *2013 IEEE Symposium on Adaptive Dynamic Programming and Reinforcement Learning (ADPRL)*. IEEE, 191–199.
- Thomas J Walsh, Ali Nouri, Lihong Li, and Michael L Littman. 2009. Learning and planning in environments with delayed feedback. *Autonomous Agents and Multi-Agent Systems* 18, 1 (2009), 83.
- Wikipedia. 2020. COVID-19 Blockade measures for epidemic areas in mainland China (in Chinese). <https://zh.wikipedia.org/w/index.php?title=2019%E5%86%A0%E7%8B%80%E7%97%85%E6%AF%92%E7%97%85%E4%B8%AD%E5%9C%8B%E5%A4%A7%E9%99%B8%E7%96%AB%E5%8D%80%E5%B0%81%E9%8E%96%E6%8E%AA%E6%96%BD&oldid=59804692>. [Online; accessed 2020-05-25].
- Suze Wilson. 2020. Pandemic leadership: Lessons from New Zealand’s approach to COVID-19. *Leadership* (2020), 1742715020929151.
- Hyun Mo Yang, Luis Pedro Lombardi Junior, and Ariana Campos Yang. 2020a. Are the SIR and SEIR models suitable to estimate the basic reproduction number for the CoViD-19 epidemic? *medRxiv* (2020).
- Zifeng Yang, Zhiqi Zeng, Ke Wang, Sook-San Wong, Wenhua Liang, Mark Zanin, Peng Liu, Xudong Cao, Zhongqiang Gao, Zhitong Mai, et al. 2020b. Modified SEIR and AI prediction of the epidemics trend of COVID-19 in China under public health interventions. *Journal of Thoracic Disease* 12, 3 (2020), 165.
- Juan Zhang, Jie Lou, Zhien Ma, and Jianhong Wu. 2005. A compartmental model for the analysis of SARS transmission patterns and outbreak control measures in China. *Appl. Math. Comput.* 162, 2 (2005), 909–924.

## A Pseudo-code of the Policy Search Algorithms

In this section, we provide the pseudo-code for the two policy search algorithms introduced in Section 4.3. The hyper-parameters used in the experiments can be found in Appendix C.2. In Algorithm 3, we describe the grid search based policy search algorithm when  $J = 3$ . In Algorithm 4, we modify the deep-Q learning algorithm to take into consideration the learned uncertainty on  $\theta$ . More details about the standard DQN can be found in (Mnih et al., 2015).

---

### Algorithm 3: Policy Search with Grid Search

---

**Input:** bounds of the search space  $u_2, u_3, U_2, U_3$ ; step sizes  $\xi_2, \xi_3$ ; number of replications  $M$ ; data  $\{O_{l,t}^I\}_{t=t_0-D}^{t_0}$  and  $\{A_{l,t}\}_{t=t_0-D}^{t_0-1}$ ; other parameters  $D, \rho_{t_0}, \omega_{l,t_0}, t_0, T, \mathcal{T}, c_l(\cdot)$   
 set  $\lambda_2 = u_2, V^* = +\infty, S_{l,t_0} = MBS(\{X_{l,t}^R\}_{t=t_0-D}^{t_0}, \{A_{l,t}\}_{t=t_0-D}^{t_0-1}, \rho_{t_0}, D)$ , and  $X_{l,t}^R = O_{l,t}^I$  for  $t \in \{t_0 - D, \dots, t_0\}$   
**while**  $\lambda_2 \leq U_2$  **do**  
     set  $\lambda_3 = \max(\lambda_2, u_3)$   
     **while**  $\lambda_3 \leq U_3$  **do**  
         set  $\lambda = (\lambda_2, \lambda_3)^T$  and the overall value  $V = 0$   
         **for**  $m = 1, \dots, M$  **do**  
             **for**  $t' = t_0, \dots, T$  **do**  
                 generate  $S_{l,t'}^G = MBS(\{X_{l,t'}^R\}_{t=t'-D}^{t'}, \{A_{l,t'}\}_{t=t'-D}^{t'-1}, \rho_{t_0}, D)$   
                 choose action  $A_{l,t'} = \pi(S_{l,t'}^G; \lambda)\mathbb{I}(t' \in \mathcal{T}) + A_{l,t'-1}\mathbb{I}(t' \notin \mathcal{T})$   
                 sample  $\theta \sim \rho_{t_0}, C_{l,t'}^A \sim c_l(A_{l,t'})$ , and  $S_{l,t'+1} \sim f(\cdot | S_{l,t'}, A_{l,t'}; \theta)$   
                 calculate  $V = V + (X_{l,t'}^S - X_{l,t'+1}^S + \omega_{l,t_0} C_{l,t'}^A)$   
             **if**  $V < V^*$  **then** update  $V^* = V$  and  $\lambda^* = \lambda$   
         set  $\lambda_3 = \lambda_3 + \xi_3$   
     set  $\lambda_2 = \lambda_2 + \xi_2$   
**Output:** optimal policy  $\hat{\pi}_{l,t_0}(\cdot; \omega_{l,t_0}) = \pi(\cdot; \lambda^*)$

---



---

### Algorithm 4: Modified deep-Q learning with experience replay and epsilon-greedy exploration for finite-horizon planning.

---

**Data:** weight  $\omega$ , posterior  $\rho_{t_0}$ , current state  $s_0$ , current decision point  $t_0$ , horizon  $T$  number of episodes  $M$ , exploration probability  $\epsilon$   
**Initialization:** set the replay buffer  $\mathcal{D}$  as empty, the action-value function  $Q(\cdot, \cdot)$  with random weights  
**for** *episode*  $e = 1, \dots, M$  **do**  
     randomly initialize with an appropriate state  $s$   
     **for**  $t = t_0, \dots, T$  **do**  
         with probability  $\epsilon / ((e + 1) / 10 + 1)$  select a random action  $a$ ; otherwise select  $a = \operatorname{argmin}_a Q((s, t), a)$   
         take action  $a$ , sample  $\theta \sim \rho_{t_0}$ , and then sample the next state  $s'$  according to the GSIR model with parameter  $\theta$   
         sample the action cost for  $a$  and calculate the weighted cost for weight  $\omega$  as  $c$   
         store transition  $(s, a, c, s', t)$  in  $\mathcal{D}$   
         sample a mini-batch  $\{(s_i, a_i, c_i, s'_i, t_i)\}$  from  $\mathcal{D}$   
         set  $y_i = c_i + \min_a Q((s'_i, t_i + 1), a)$  if  $s'_i$  is not terminal, and set  $y_i = c_i$  otherwise  
         perform a gradient descent step on  $\{(s_i, t_i), y_i\}$   
         set  $s' = s$   
**Result:** optimal policy  $\hat{\pi}_{t_0}(\cdot; \omega) = \operatorname{argmin}_a Q((\cdot, t_0), a; \omega)$  and the recommended action  $\hat{\pi}_{t_0}(s_0; \omega)$

---

## B Robustness analysis results

In Figure B, we report the robustness analysis results. The experiment details can be found in Appendix C.4. In subplot (a), we present results when the true data generation process is a generalized Susceptible-Exposed-Infected-Removal model (SEIR) model. As expected, compared with results under the GSIR model, the performance of the proposed method under this setting slightly deteriorates. However, in general, the method still over-performs the other fixed policies, and also provides more options with a clear trade-off.

In subplot (b) and (c), we present results when different hyper-parameters are used. We present results for the threshold-based policy class. Results for the DQN-based methods are similar and omitted, for ease of presentation. These prior parameters turn out to have little importance in the long run, because their effects get washed out quickly by the observed data. The findings for the other prior parameters are similar.

## C Details of the experiments

### C.1 Dataset and hyper-parameters

We obtain the counts of cumulative confirmed cases  $O_{l,t}^I$  from (Lab, 2020) with irregular records imputed by the average of their neighbors. For each region  $l$ , we collect its annual gross domestic product (GDP)  $G_l$  and population  $M_l$  from a Chinese demographic dataset<sup>1</sup>. The original mobility data collected from the online platform Baidu Qianxi<sup>2</sup> includes  $m_{l,t}^{20}$ , the mobility of people in city  $l$  on day  $t$  in 2020, and  $m_{l,t}^{19}$ , the value for the same date in 2019, aligned by the lunar calendar. We define  $r_{l,t} = 1 - m_{l,t}^{20}/m_{l,t}^{19}$  to measure the ratio of human mobility loss due to  $A_{l,t}$ . The fitted distributions for the intervention cost function are  $C_2 \sim \mathcal{N}(0.368, 0.239^2)$  and  $C_3 \sim \mathcal{N}(0.484, 0.181^2)$ . As for the action data, we collect the date ranges for different control measures claimed by Chinese local governments. The date ranges for action 1 and 2 as well as the starting dates for action 3 are collected from (Wikipedia, 2020). The ending dates for action 3 are manually collected from the local government websites or their social media accounts. We use the estimates for SARS (Mkhatshwa and Mummert, 2010) to set the priors for the disease features, specifically, we set  $\gamma \sim \text{Beta}(178.89, 2000)$  and  $\beta_1 \sim \text{Gamma}(517.41, 2000)$ . As for  $\beta_2$  and  $\beta_3$ , similar with the assumptions in (Ferguson et al., 2020), we assume the two measures reduce the infection rate by 80% and 90% respectively, and therefore use  $\beta_2 \sim \text{Gamma}(103.48, 2000)$  and  $\beta_3 \sim \text{Gamma}(51.74, 2000)$ .

### C.2 Implementation details

In our experiments, for the grid search algorithm, the number of rollout replications is set as  $M = 100$ . We run the grid search algorithm from coarse grids to finer grids to save computational cost. The schedule is listed in Table 2. In general, the larger the search spaces and the smaller the step sizes, the better the performance will be. In consideration of the importance of this application and the relatively lightweight computation, in real applications, we can choose the search spaces as large enough and step size as small enough. For DQN, we use a dense network of 5 layers, with 32 nodes per layer, to model the Q-function. The activation function is picked as relu and the optimizer is set as Adam. The learning rate is fixed as 0.0002 and the parameter for epsilon-greedy is set as  $\epsilon = 0.1$ .

Table 2: Search space and step sizes for the grid search in each round.  $\lambda_1^i$  and  $\lambda_2^i$  are the output from the  $i$ -th round.

Round	$u_2$	$u_3$	$U_2$	$U_3$	$\xi_2$	$\xi_3$
1	0	300	50	0	100	200
2	$\max(0, \lambda_1^1 - 50)$	$\lambda_1^1 + 50$	5	$\lambda_2^1 - 200$	$\lambda_2^1 + 200$	20
3	$\max(0, \lambda_1^2 - 5)$	$\lambda_1^2 + 5$	1	$\lambda_2^2 - 20$	$\lambda_2^2 + 20$	4
4	$\max(0, \lambda_1^3 - 1)$	$\lambda_1^3 + 1$	0.25	$\lambda_2^3 - 4$	$\lambda_2^3 + 4$	1
5	$\max(0, \lambda_1^4 - 0.25)$	$\lambda_1^4 + 0.25$	0.01	$\lambda_2^4 - 1$	$\lambda_2^4 + 1$	0.2

### C.3 Validity of the simulation environment

We apply a leave-one-out cross-validation procedure to show that our simulation environment is close to the real data generation process. Specifically, for  $l = 1, \dots, 6$ , we follow the steps:

1. estimate the environmental parameter  $\theta$  as  $\hat{\theta}_l$ , using all data until day 61 of cities in  $\{1, \dots, 6\} \setminus \{l\}$ .
2. for city  $l$ , based on  $\hat{\theta}_l$ , we predict its counts of the cumulative infected cases from day 12 to day 120, following the observed actions in the data. Denote the estimate for day 120 as  $\hat{X}_{120,l}^R$ .
3. calculate the approximation error by  $\epsilon_l = |\hat{X}_{120,l}^R - O_{120,l}^I|/O_{120,l}^I$ , where  $O_{120,l}^I$  is the observed cumulative infected count for city  $l$  until day 120.

<sup>1</sup><https://www.hongheiku.com>

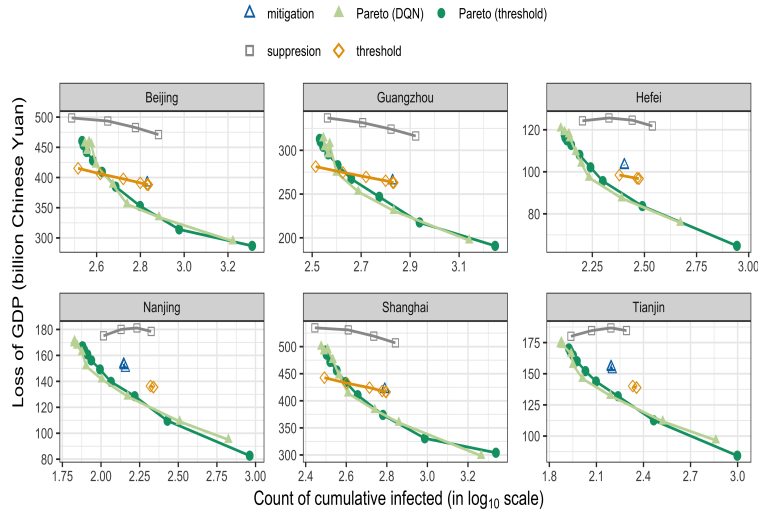
<sup>2</sup><http://qianxi.baidu.com>

The average error ratio  $\sum_{l=1}^6 \epsilon_l / 6 = 0.18$  indicates that the environment is a relatively valid proxy for the real data generation process, which supports the fairness of our comparison with the behaviour policy. It also partially supports that these regions are similar.

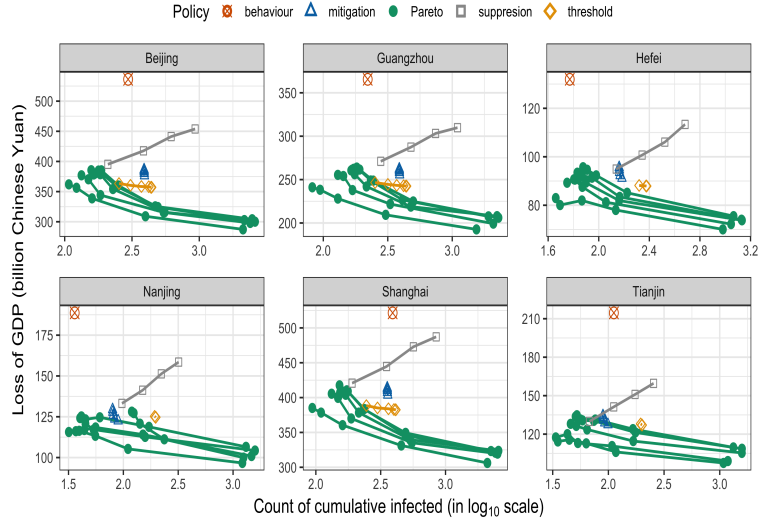
#### C.4 Setting for the robustness analysis

The Susceptible-Exposed-Infected-Removal model (SEIR) model is another commonly used compartmental model, which adds one additional exposed compartment to the SIR model (Tang et al., 2020). We generalize the SEIR model in a similar way as the GSIR model, by including the action effects into consideration to set the infection rate  $\beta$ . The transition from the susceptible compartment to the exposed compartment is assumed to follow a binomial distribution with parameter  $\alpha$ . According to (Yang et al., 2020b), we set the incubation rate  $\alpha$  as  $1/7$ . The other parameters are kept the same with Section 5.3. Since the exposed compartment is typically latent, the number of individuals in this compartment on the beginning date can not be set based on the real data as the other compartments. For experiment purpose, we set the number to be the same as the number in the infectious compartment.

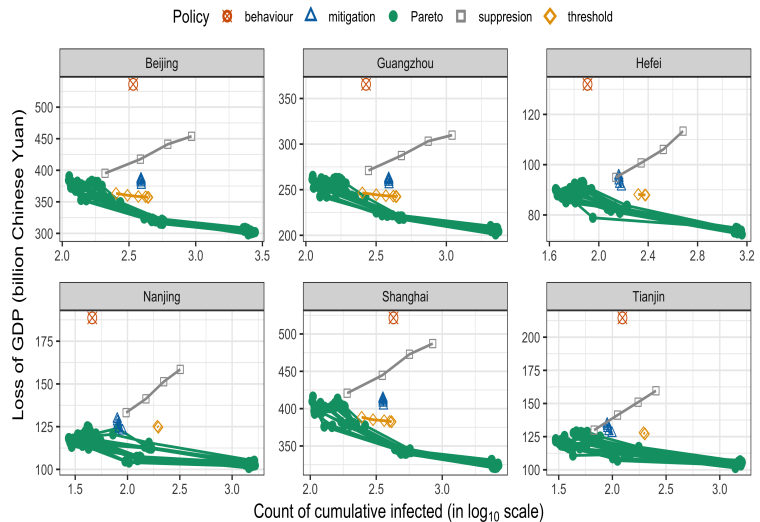
For sensitiveness to hyper-parameters, we considered two settings: (1)  $D = 7, 8, 9, 10, 11$ , with the other hyper-parameters fixed; (2)  $\{(\mu_2, \mu_3) : \mu_3 \in \{0.05, 0.1, 0.15, 0.2\}, \mu_2 - \mu_3 \in \{0.05, 0.1, 0.15, 0.2\}\}$ , with the other hyper-parameters fixed. Recall that we define  $\mu_j = \beta_j / \beta_1$  and use it to set the prior for  $\beta_j$ . The other settings are kept the same with Section 5.3, except for that we only run 25 replications for the proposed algorithm to save computation.



(a) Results when the data generation model is the generalized SEIR model.



(b) Results for different values of  $D$ .



(c) Results for different values of  $\mu_1$  and  $\mu_2$ .

Figure 7: Robustness analysis results